

An artificial viscosity model for 3D simulations with Vortex Methods

C. Mimeau*, G.-H. Cottet** and I. Mortazavi*
Corresponding author: chloe.mimeau@cnam.fr

* M2N Laboratory, Conservatoire National des Arts et Métiers, Paris, FRANCE

** LJK Laboratory, Université Grenoble-Alpes, Grenoble, FRANCE.

1 Introduction

Vortex methods discretize the flow quantities on particles which move according to the flow dynamics. They are therefore ideal to handle vortex-dominated flow simulations, like flows past bluff-bodies, airfoils, propellers, turbine profiles as well as complex internal configurations or jet flows.

In the present work, we use a remeshed vortex method with penalization in order to simulate three-dimensional incompressible bluff body flows. This approach, based on a vorticity ($\boldsymbol{\omega}$)-velocity (\mathbf{u}) formulation of the Navier-Stokes equations, combines the robustness of vortex methods and the flexibility of penalization methods to impose boundary conditions on the obstacle through the introduction of an underlying Cartesian grid. This numerical method has been successfully used in the context of Direct Numerical Simulations of flow past bluff bodies.

Due to the immersed boundary approach, one of the main limitation of such method arises when increasing the Reynolds number. In order to be able to consider higher Reynolds numbers without dealing with prohibitive mesh sizes, we adopt in this work a bi-level approach. The latter consists in transporting the vorticity field $\boldsymbol{\omega}$ on a fine grid with a filtered velocity field \mathbf{u} resolved on a coarse mesh. For this purpose we propose an artificial viscosity model for vortex methods.

2 Direct Numerical Simulations with a remeshed Vortex Method

2.1 Governing equations and discretization method

The modeling of incompressible 3D flows around obstacles is realized in this work using a remeshed Vortex Method (VM) coupled with an immersed boundary approach called the Brinkman penalization method. The governing Brinkman-Navier-Stokes equations are expressed in their velocity(\mathbf{u})-vorticity($\boldsymbol{\omega}$) fomulation [1]:

$$\frac{\partial \boldsymbol{\omega}}{\partial t} + (\mathbf{u} \cdot \nabla) \boldsymbol{\omega} - \operatorname{div}(\boldsymbol{\omega} : \mathbf{u}) = \nabla \times \left(\lambda \chi_b (\mathbf{u}_b - \mathbf{u}) \right) + \frac{1}{Re} \Delta \boldsymbol{\omega} \quad \text{in } D, \quad (1)$$

$$\Delta \mathbf{u} = -\nabla \times \boldsymbol{\omega} \quad \text{in } D, \quad (2)$$

where Re denotes the Reynolds number, χ_b represents the characteristic function that yields 0 in the fluid and 1 in the solid body, \mathbf{u}_b indicates the rigid body velocity and λ is the non-dimensional penalization parameter. One can distinguish in Eq. (1) the advection term $(\mathbf{u} \cdot \nabla) \boldsymbol{\omega}$, the stretching term $\operatorname{div}(\boldsymbol{\omega} : \mathbf{u})$ expressed in its conservative form, the vorticity penalization term $\nabla \times (\lambda \chi_b (\mathbf{u}_b - \mathbf{u}))$ and the diffusion term $\Delta \boldsymbol{\omega} / Re$. The Poisson equation (2) allows to recover the velocity field \mathbf{u} from the vorticity field $\boldsymbol{\omega}$. This system of equations has to be complemented by appropriate boundary conditions at artificial boundaries.

To discretize the penalized vorticity equations (1)-(2) we use in this work a remeshed vortex method. The flow is discretized onto particles that carry the vorticity and the resolution of the governing equations is based on a fractional step algorithm, which consists at each time step to successively solve the different equations (Table 1). The advection equation is solved in a Lagrangian way and after each advection step,

the particles are remeshed on a Cartesian grid. Eulerian grid-based methods are then employed to solve the stretching, diffusion, penalization and Poisson equations.

	Fractional steps	Time discretization	Space discretization
1) Poisson equation	$\Delta \mathbf{u} = -\nabla \times \boldsymbol{\omega}$	-	spectral method (grid)
2) Penalization	$\partial_t \boldsymbol{\omega} = \nabla \times \left(\lambda \chi_b (\mathbf{u}_b - \mathbf{u}) \right)$	implicit Euler scheme	4 th order centered FD (grid)
3) Stretching	$\partial_t \boldsymbol{\omega} = \text{div}(\boldsymbol{\omega} : \mathbf{u})$	RK3 scheme	4 th order centered FD (grid)
4) Diffusion	$\partial_t \boldsymbol{\omega} = \frac{1}{Re} \Delta \boldsymbol{\omega}$	implicit Euler scheme	spectral method (grid)
5) Advection	$\partial_t \boldsymbol{\omega} + (\mathbf{u} \cdot \nabla) \boldsymbol{\omega} = 0$	RK2 scheme	$\Lambda_{4,2}$ remeshed VM (particles)
6) Adaptive time step	$\Delta t_{\text{adapt}} = \frac{\text{LCFL}}{\ \nabla \mathbf{u}\ _{\infty}}$ (LCFL < 1)	-	4 th order centered FD (grid)

Table 1: Fractional step algorithm used to solve the penalized vorticity equations (1)-(2) at each time step.

2.2 Validation

Flow past a sphere is a common benchmark to validate the accuracy of a numerical method and to prove its capability to correctly model 3D bluff body flows. The validation simulation is performed at $Re = 1000$ setting the grid step to $h = 0.01$. The adaptive time step, calculated with $\text{LCFL} = 1/8$, returns a value roughly equal to $\Delta t = 0.005$, which corresponds to a CFL number equal to 0.6.

A plot of the time average streamwise velocity u_x along the centerline is given in Figure 1a. The results obtained with the present method are compared to those of [2] along with the experimental data of [3] at $Re = 960$. It can be seen that the length of the recirculation zone, characterized by negative u_x values, obtained in the present case (1.5 diameters) is similar to the one obtained in [2] (approximately 1.7 diameters). Furthermore, the u_x values obtained in the far field (i.e. for $x/d > 2$) are in a very good agreement with other numerical [2] and experimental studies [3].

Concerning the time evolution of force coefficients, Figure 1b shows that the early time evolution of the drag coefficient C_D and the vertical lift coefficient C_L coincide with the one found by [4]. Moreover, the mean value of the drag coefficient C_D obtained in the present study is 0.485, which coincides well with the numerical values reported by [5] and [6], respectively equal to 0.46 and 0.478.

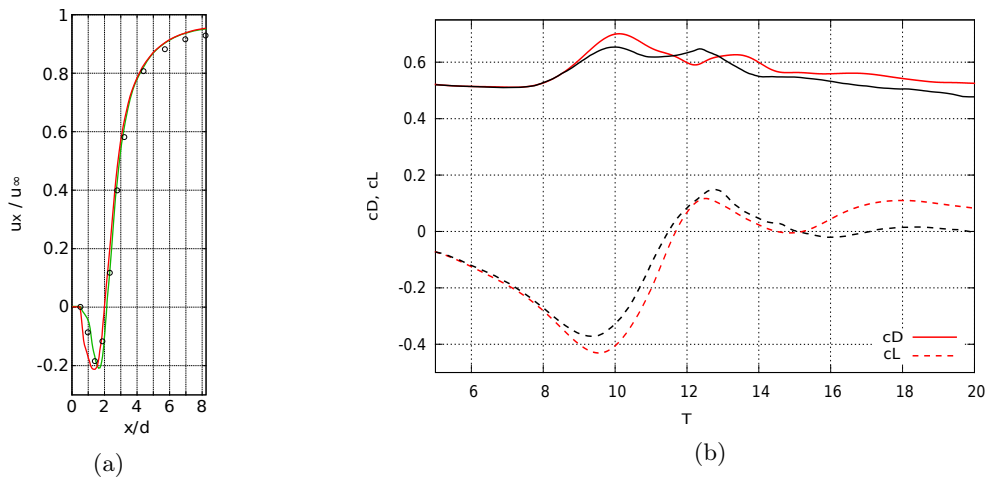


Figure 1: Flow past a sphere at $Re = 1000$: (a) Average streamwise velocity u_x along the x -axis: comparison of the present results (red curve) with numerical results [2] (green curve) and experimental data [3] at $Re = 960$ (black circles). (b) C_D (solid lines) and C_L (dashed lines) time evolution: comparison of the present results (red curves) with [4] (black curves).

2.3 DNS results for flow past a hemisphere

Hemispherical bodies correspond to configurations that may be used in several engineering applications. Moreover, due to the presence of a flat back wall with sharp edges, the flow past a hemisphere is a steep problem. The present simulation of flow past a hemisphere is performed at $Re = 1000$.

The time history of the force coefficients is reported in Figure 2a. It shows that from $T \simeq 55$ the wake becomes chaotic and is characterized by important and non-periodic variations of the side lift coefficient C_S .

Three-dimensional representations of the turbulent wake is given in Figure 2b(top) at $T = 100$. Figure 2b(bottom) also reports the time average of the vorticity magnitude calculated between $T = 70$ and $T = 110$, showing the chaotic feature of the wake. In particular, we remark that a large recirculation area with low vorticity values exists behind the hemisphere, followed by an important zone characterized by high vorticity values.

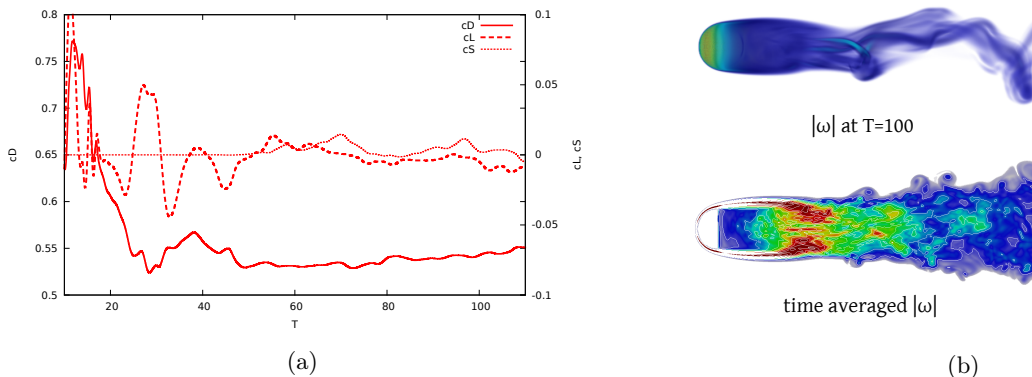


Figure 2: DNS results for flow past a 3D hemisphere at $Re = 1000$.

Further results concerning the validation of the present method and its application to other simulations of 3D flows around bluff bodies may be found in [7].

3 Eddy viscosity model for a bi-level approach

When dealing with large Reynolds number flows, the computational cost induced by the present DNS approach becomes prohibitive, even unaffordable. To overcome this limit we propose a bi-level method, which may be seen as a LES approach, consisting in transporting the vorticity field on a fine grid with a filtered velocity, resolved on a coarse mesh.

The eddy viscosity model used in this section to perform bi-level simulations was introduced by [8] and is based on the vortex methods framework.

3.1 An eddy viscosity model for Vortex methods

Let us consider the 3D velocity-vorticity formulation of the Euler equations :

$$\frac{\partial \boldsymbol{\omega}}{\partial t} + \text{div}(\mathbf{u} : \boldsymbol{\omega}) - \text{div}(\boldsymbol{\omega} : \mathbf{u}) = 0 \quad \text{in } D, \quad (3)$$

$$\text{div}(\mathbf{u}) = 0 \quad \text{in } D, \quad (4)$$

$$\mathbf{u} \longrightarrow \mathbf{u}_\infty \quad \text{at infinity} \quad (5)$$

To solve these equations, pure Lagrangian Vortex Methods consist in representing the vorticity field by a distribution of particle which carry the local values of the circulation Γ . Generally, a continuous vorticity field is recovered with vortex blob method, using the mollifying function ζ_ε of radius ε instead of the Dirac distribution :

$$\boldsymbol{\omega}_\varepsilon = \sum_p \Gamma_p \zeta_\varepsilon(\mathbf{x} - \mathbf{x}_p),$$

The regularized velocity field \mathbf{u}_ε is calculated from the Biot-Savart law, with the Poisson kernel \mathbf{K} :

$$\begin{aligned} \mathbf{u}_\varepsilon &= \mathbf{u}_\infty + \mathbf{K}_\varepsilon \star \boldsymbol{\omega}_\varepsilon \\ \mathbf{K}_\varepsilon &= \mathbf{K} \star \zeta_\varepsilon \end{aligned} \quad (6)$$

Finally, it turns out that vortex blob method satisfies the regularized Euler equations :

$$\frac{\partial \bar{\boldsymbol{\omega}}}{\partial t} + \operatorname{div}(\bar{\mathbf{u}} : \bar{\boldsymbol{\omega}}) - \operatorname{div}(\bar{\boldsymbol{\omega}} : \bar{\mathbf{u}}) = 0 \quad (7)$$

where the notations $\boldsymbol{\omega}_\varepsilon$ and \mathbf{u}_ε have respectively been replaced by $\bar{\boldsymbol{\omega}}$ and $\bar{\mathbf{u}}$ to denote the regularized fields. Equation (7) is equivalent to :

$$\frac{\partial \bar{\boldsymbol{\omega}}}{\partial t} + \operatorname{div}(\bar{\mathbf{u}} : \bar{\boldsymbol{\omega}}) - \operatorname{div}(\bar{\boldsymbol{\omega}} : \bar{\mathbf{u}}) = E, \quad (8)$$

where E represents the truncation error.

E intrinsically involves the tensor $\bar{\mathbf{u}} \bar{\boldsymbol{\omega}} - \bar{\boldsymbol{\omega}} \bar{\mathbf{u}}$, which is reminiscent to the subfilter scale stress tensor τ_{ij} in LES methods.

In the vortex method framework, no closure model is needed to express this tensor. Based on the error E expression, an evaluation of the enstrophy production allows to directly derive an eddy viscosity model. According to [8], the evaluation of enstrophy production in 2D is derived from the expression of the 2D truncation error E and is expressed as :

$$\frac{d}{dt} \int \omega^2 d\mathbf{x} = - \iint [\omega(\mathbf{x}) - \omega(\mathbf{y})]^2 [\mathbf{u}(\mathbf{x}) - \mathbf{u}(\mathbf{y})] \cdot \nabla \zeta_\varepsilon(\mathbf{x} - \mathbf{y}) d\mathbf{x} d\mathbf{y}, \quad (9)$$

This expression means that when

$$[\mathbf{u}(\mathbf{x}) - \mathbf{u}(\mathbf{y})] \cdot \nabla \zeta_\varepsilon(\mathbf{x} - \mathbf{y}) < 0, \quad (10)$$

one has a positive enstrophy budget, which can be interpreted as the indication of backscatter. Therefore, [8] proposes the following 2D anisotropic viscosity model for vortex methods, based on the cancellation of the enstrophy production only in the directions where condition (10) is satisfied :

$$\frac{d\omega_p}{dt} = \sum_q \mathbf{v}_q \{ [\mathbf{u}(\mathbf{x}_p) - \mathbf{u}(\mathbf{x}_q)] \cdot \nabla \zeta_\varepsilon(\mathbf{x}_p - \mathbf{x}_q) \}_+ (\omega_p - \omega_q), \quad (11)$$

where $a_+ = \max(0, a)$.

This 2D model has been extended to 3D in [9]. Based on this work, we replace the step 3) of our remeshed vortex method fractional step algorithm presented in the first sections of this paper (Table 1) by :

$$\frac{d\boldsymbol{\omega}_p}{dt} = \operatorname{div}(\boldsymbol{\omega}_p \mathbf{u}_p) + C \Delta^{-4} \sum_q \mathbf{v}_q \left| [\mathbf{u}(\mathbf{x}_p) - \mathbf{u}(\mathbf{x}_q)] \cdot [\mathbf{x}_p - \mathbf{x}_q] g(|\mathbf{x}_p - \mathbf{x}_q|) \right| (\boldsymbol{\omega}_p - \boldsymbol{\omega}_q), \quad (12)$$

where Δ will be the filter size used to filter the velocity field and where $\nabla \zeta_\varepsilon \left(\frac{\mathbf{x}_p - \mathbf{x}_q}{\Delta} \right)$ is defined in this case by :

$$\nabla \zeta_\varepsilon \left(\frac{\mathbf{x}_p - \mathbf{x}_q}{\Delta} \right) = C \frac{[\mathbf{x}_p - \mathbf{x}_q]}{\Delta} g(|\mathbf{x}_p - \mathbf{x}_q|),$$

with g a function decaying at infinity and C a constant to adjust in the model.

3.2 Numerical results

Model (12) has been applied to the Taylor-Green vortex benchmark, which constitutes a relevant three-dimensional test case to investigate the generation of small-scale vorticity. The simulations are performed in a periodic cubic box of side length $L = 2\pi$ and initialized with the following smooth condition:

$$\begin{aligned} u_x(\mathbf{x}, t = 0) &= \sin(x) \cos(y) \cos(z) \\ u_y(\mathbf{x}, t = 0) &= -\cos(x) \sin(y) \cos(z) \\ u_z(\mathbf{x}, t = 0) &= 0 \end{aligned} \tag{13}$$

The Reynolds number of the flow is set to $Re = 1600$. The bi-level simulations presented here were obtained by using the eddy viscosity model (12), with a vorticity field $\boldsymbol{\omega}$ fully resolved on a fine mesh of step h while the small scales of the velocity field \mathbf{u} are filtered with the following spectral cutoff filter :

$$f_{k_\Delta}(|\mathbf{k}|) = \begin{cases} 1 & \text{if } |\mathbf{k}| \leq k_\Delta = \frac{\pi}{\Delta} \\ 0 & \text{otherwise,} \end{cases}$$

where $\Delta = nh$ is the filter size, with $n \in \mathbb{N}^*$.

Figure 3 compares the evolution of enstrophy obtained by van Rees et. al in [10] with DNS using a 512^3 resolution (red curve) and the one obtained with the proposed artificial viscosity model taking a $512^3 - 128^3$ resolution, and setting $C = 0.04$ (black) curve. The figure also shows the norm of vorticity field obtained with the bi-level approach at the initial time and at the time $T = 8.9$ when the viscous dissipation of kinetic energy reaches a peak. It emerges from the curves that the artificial viscosity model (12) manages to capture the correct behavior of the flow, especially between $T = 8$ and $T = 10$ when the energy dissipation due to molecular viscosity reaches its maximum. Figure 4 shows the contours of the vorticity norm obtained at $T = 8$ in the YZ plane at $x = 0$ (center of the box) according to model (12) with $C = 0.04$, using a $256^3 - 64^3$ (left) and a $512^3 - 128^3$ (center) resolution. They are compared to the contours obtained with DNS [10] with a 512^3 resolution (right). These figures show that the contours obtained with the proposed artificial viscosity model taking a $512^3 - 128^3$ resolution are very close in a qualitative point of view to the one given by the Direct Numerical Simulations of [10], which confirms the capability of the proposed model to correctly take into account the physics of the problem. The good agreement observed between the present results and the one obtained from Direct Numerical Simulations confirms the capability of the proposed artificial viscosity model to capture the large scales of the flow and thus to account for the global behavior of the flow.

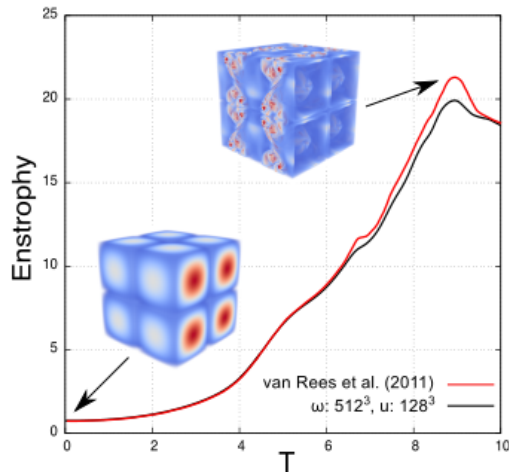


Figure 3: Bi-level results: enstrophy of a Taylor-Green vortex at $Re = 1600$ with a $512^3 - 128^3$ resolution compared to the DNS result obtained by [10] with a 512^3 resolution.

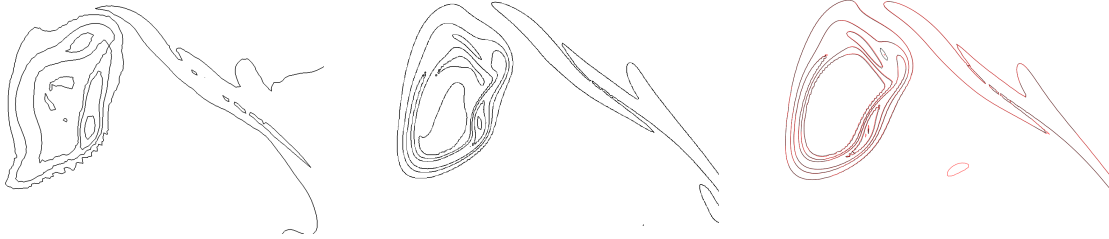


Figure 4: Contours of vorticity norm at $T = 8$ in the YZ plane at $x = 0$ in a 2π -long cubic domain obtained with the present eddy viscosity model with a $256^3 - 64^3$ resolution (left) and a $512^3 - 128^3$ resolution (center). They are compared to the DNS results obtained by [10] with a 512^3 resolution (right).

References

- [1] N. Kevlahan and J. M. Ghidaglia. Computation of turbulent flow past an array of cylinders using a spectral method with Brinkman penalization. *Eur. J. Mech.*, B 20:333–350, 2001.
- [2] A. Tomboulides and A. Orszag. Numerical investigation of transitional and weak turbulent flow past a sphere. *J. Fluid Mech.*, 416:45–73, 2000.
- [3] J.S. Wu and G.M. Faeth. Sphere wakes in still surroundings at intermediate Reynolds numbers. *AIAA J.*, 31(8):1448–1455, 1993.
- [4] P. Ploumhans, G. S. Winckelmans, J. K. Salmon, A. Leonard, and M. S. Warren. Vortex methods for direct numerical simulation of three-dimensional bluff body flows: Applications to the sphere at $Re = 300, 500$ and 1000 . *J. Comput. Phys.*, 178:427–463, 2002.
- [5] E.K.W. Poon, G. Iaccarino, A.S.H. Ooi, and M. Giacobello. Numerical studies of high Reynolds number flow past a stationary and rotating sphere. *Seventh International Conference on CFD in the Minerals and Process Industries CSIRO, Melbourne, Australia*, 2009.
- [6] R. Campregher, J Militzer, S.S Mansur, and A. da Silveira Neto. Computations of the flow past a still sphere at moderate Reynolds numbers using an immersed boundary method. *J. of the Braz. Soc. of Mech. Sci. & Eng.*, 31(4):344–352, 2009.
- [7] C. Mimeau, G.-H. Cottet, and I. Mortazavi. Direct numerical simulations of three-dimensional flows past obstacles with a vortex penalization method. *Comp & Fluids*, 136:331–347, 2016.
- [8] G.-H. Cottet. Artificial viscosity models for vortex and particle methods. *J. Comput. Phys.*, 127:199–208, 1996.
- [9] G.-H. Cottet. Anisotropic subgrid-scale numerical schemes for large eddy simulation of turbulent flows. *Unpublished report*, 1997.
- [10] W. M. van Rees, A. Leonard, D.I. Pullin, and P. Koumoutsakos. A comparison of vortex and pseudo-spectral methods for the simulation of periodic vortical flows at high reynolds numbers. *J. Comput. Phys.*, 230(8):2794–2805, 2011.